



# Prospective applications of transition metal-based nanomaterials

Liwei Xiong<sup>1</sup>, Yukang Fu<sup>1</sup>, Yongxin Luo<sup>2</sup>, Youshan Wei<sup>1</sup>, Ze Zhang<sup>1</sup>, Chaoguo Wu<sup>1</sup>, Sicheng Luo<sup>1</sup>, Gang Wang<sup>1</sup>, David Sawtell<sup>3</sup>, Kefeng Xie<sup>4</sup>, Tao Wu<sup>5</sup>, Dong Ding<sup>6</sup>, Liang Huang<sup>2,a)</sup>

<sup>1</sup>Hubei Key Laboratory of Plasma Chemistry and Advanced Materials, Key Laboratory of Novel Biomass-Based Environmental and Energy Materials in Petroleum and Chemical Industry, Wuhan Institute of Technology, Wuhan 430205, China

<sup>2</sup>Wuhan National Laboratory for Optoelectronics, Huazhong University of Science and Technology, Wuhan, Hubei 430074, People's Republic of China

<sup>3</sup>Faculty of Science and Engineering, Manchester Metropolitan University, Chester Street, Manchester M1 5GD, UK

<sup>4</sup>College of Chemistry and Chemical Engineering, Lanzhou Jiaotong University, Lanzhou 730070, People's Republic of China

<sup>5</sup>State Key Laboratory of Fine Chemicals, School of Chemical Engineering, Dalian University of Technology, Dalian 116024, People's Republic of China

<sup>6</sup>Energy & Environmental Science and Technology, Idaho National Laboratory, Idaho Falls, ID 83401, USA

<sup>a)</sup>Address all correspondence to this author. e-mail: huangliang421@hust.edu.cn

Liwei Xiong, Kefeng Xie, Tao Wu, Dong Ding, Liang Huang are the guest editors of this issue.

Received: 24 May 2022; accepted: 29 June 2022; published online: 11 July 2022

**Transition metal-based nanomaterials (TMNs), including metal oxides, metal nitride, metal carbide, metal hydroxide, and metal sulfide, have recently arisen as robust and highly efficient materials for energy storage and conversion. Owing to extraordinary advantages over the semiconducting/insulating ones (in terms of fast reaction kinetics, rapid electrical transport, and intrinsically high activity) combined with the high natural abundance, this class of materials is progressively developed toward commercial applications. This article gives an overview of recent research works on transition metal-based nanomaterials in terms of fundamental applications in energy conversion and energy storage. Additionally, the current structure and properties of transition metal-based nanomaterials have been summarized for the application of energy storage systems which can alleviate the challenges that currently exist in energy conversion. Overall, this review aims to provide a new vision for alleviating the current energy crisis, and environmental problems in the future period, and find the direction and breakthrough for the next energy transformation.**

## Introduction

In recent years, the energy crisis and environmental degradation have become an issue that all of humanity has to face up to. At the UN Climate Change Conference in Glasgow in 2021, it was proposed to reduce the use of fossil fuels and subsidize increased investment in clean energy, which has undoubtedly accelerated the development of clean and sustainable energy sources. However, most renewable energy sources today do not have a stable and sustainable output, and the storage and conversion of renewable energy is currently a major concern [1]. The potential of transition metal-based nanomaterials (TMNs) for energy storage and conversion is of great interest. When nanotechnology emerged, it was realized that such transition

metal-based compounds might have extraordinary properties at the nanoscale. As a result, over the past few decades, scholars have continuously developed various types of transition metal-based nanomaterials, such as transition metal oxides, transition metal nitrides, transition metal carbides, transition metal sulfides, and so on [2]. But at the root of the problem, such a wide range of applications and excellent properties are inextricably linked to their special structures. For example, transition metal nitrides are compounds in which nitrogen atoms are interstitially bonded with transition group metals [3]. Under certain conditions of nitridation, the ordered nitridation of oxide precursors (or single-crystal transition metals) through “local structural reactions” can produce nanostructures with a

high specific surface area [4]. From a crystal structure point of view, due to the insertion of the chemically bonded atoms, the separation distance between the metal atoms increases due to the insertion of the atoms, the metal lattice expands, and the forces between the metal atoms are weakened. This leads to a corresponding contraction of the metal d-energy band and a change in the Fermi energy level. Therefore, defect engineering, alloying structures, atomic doping, and heterojunctions are used to modify the properties of transition metal-based nanomaterials [5–8].

The structure of a material determines its properties. For zero-dimensional (0 D) transition metal-based nanomaterials, thanks to the small size, surfaces at all locations are accessible to the reactants, there is no significant solid-state diffusion, and they can be integrated into multiple systems. A very recent example is the use of nitrogen-containing glasses to prepare fine ZrN nanoparticles at moderate temperatures (800 °C), a method that effectively prevents grain aggregation and grain growth, thereby achieving an increased active surface area [9]. For one-dimensional (1D) transition metal-based nanomaterials, for example, nanowires and nanorods, Han et al. have successfully synthesized ultra-long single-crystal tin nanowires by a new CVD method [10], which, although only nitrides have been investigated, offers a relatively new approach to synthesis. Two-dimensional (2D) transition metal carbides, nitrides, and carbon-nitrides, also known as MXenes, have attracted the attention and interest of the scientific community due to their superior mechanical strength and flexibility, physical/chemical properties, and a variety of exciting functions [11]. Among them, the molten salt-catalyzed synthesis of two-dimensional layered transition metal nitrides for efficient hydrogen precipitation and the use of chemical vapor deposition to synthesize two-dimensional structured transition metal-based nanomaterial electrodes by heating with the corresponding precursors ( $C_2H_2$ , B powder and  $NH_3$ ) are the mainstream preparation routes today [12, 13]. Large area fabrication is still being explored, and if large area wafer level growth is achieved, its application fields will be further expanded (e.g., transistors, solar cells). The development of 3D hierarchically structured transition metal-based nanomaterials is of great interest for commercial electrodes with thicknesses in excess of the micron level and reduced activity due to high mass loading. To date, various methods have been developed. Combining the properties of transition metal materials with the new possibilities brought by nanostructures, many people have begun to explore the research and application of such materials in various fields [14–17].

Based on the corresponding small size, high specific surface area, the quantum effect, and their unique electronic structure of nanomaterials, TMNs can be used in electrolytic water for hydrogen production, metal–oxygen batteries, supercapacitors, fuel cells, and lithium batteries. In the case of electrolytic water,

there are two main processes: hydrogen and oxygen precipitation, which will be electrolyzed out from water at the cathode and anode under the condition of electricity. As transition metal-based nanomaterials (TMNs) tend to have a relatively large dispersion and more exposed active centers, this directly increases their catalytic activity as electrochemical catalysts and also greatly improves their corrosion resistance in the case of nanomaterials with oxygen, nitrogen, carbon, and sulfur atoms filling the metal interstices [18]. In the field of energy storage, transition metal-based nanomaterials are widely used in energy storage, including supercapacitors, because of their high specific surface area, electrical conductivity, and chemical inertness. Similarly, because of their special material and electronic structures, TMNs have excellent catalytic properties in various types of batteries by catalyzing anodic oxidation and cathodic reduction, thus breaking through the slow reaction kinetics to limit the performance of batteries [3, 19–21]. In addition to the several application fields mentioned above, transition metal-based nanomaterials can also be used in photoemission and photovoltaic devices, ultra-high temperature ceramics, electromagnetic wave absorbing materials, luminescent host material, electrocatalysts, and so on [22–26]. As far as current research is concerned, it is difficult to adapt single nanoparticles to such a complex application environment, whether transition metal-based nanomaterials are used for decomposing water, new batteries, or supercapacitors. In recent years, two-dimensional nanofilms or nanosheets have been used to catalyze, or composite nanoparticles with supports, or directly synthesis three-dimensional structures and mesoporous materials. Transition metal-based nanomaterials exhibit excellent catalytic and electrical properties among similar compound nanomaterials due to their special crystal structure and have shown great commercial potential for catalytic properties of noble metal catalysts due to the availability and low cost of raw materials.

### TMNs for water splitting

The electrolysis process of water is composed of two parts: the oxygen evolution reaction of the anode and the hydrogen evolution reaction of the cathode. It needs a high efficiency and stable electrocatalyst to reduce the overpotential during the reaction process, thereby speeding up the water electrolysis reaction and reducing the electrical energy loss during the water splitting. TMNs have a wide range of applications in the field of catalysts in the field of water splitting.

For example, heterostructure can be formed by constructing transition metal sulfide and transition metal hydroxide materials as efficient catalysts in the process of water splitting. This heterostructure not only retains the inherent characteristics of each component but also maximizes the synergistic

effect of the two components in the heterostructure. Its engineering exhibits many unique structural advantages, such as confinement effects, strain effects, interfacial bonding effects, and synergistic effects [27].

Song et al. [28] constructed a heterostructure of MoS<sub>2</sub> and layered double hydroxide (LDH) as a catalyst for basic HER. Due to the synergistic effect between the two, the hydrogen evolution reaction intermediates \*H and \*OH were more easily absorbed and desorption by the interface between MoS<sub>2</sub> and LDH, further accelerating the HER kinetics and obtaining better hydrogen evolution performance. Xiong et al. [29] reported that MoS<sub>2</sub>/NiFe-LDH superlattice also achieved efficient overall water splitting. It exhibits low overpotentials of 210 and 110 mV at 10 mA cm<sup>-2</sup>, respectively, for oxygen evolution reaction (OER) and alkaline hydrogen evolution reaction (HER), which are superior to MoS<sub>2</sub>/graphene and NiFe-LDH/graphene superlattice, respectively. The excellent performance was attributed to the optimal adsorption energies of the HER and OER intermediates on the MoS<sub>2</sub>/NiFe-LDH superlattice, which originates from the strong electronic coupling effect at the interface.

Liu et al. [30] reported that NiCo<sub>2</sub>S<sub>4</sub>@NiFe-LDH heterostructure catalysts on nickel foam enhanced the overall water-splitting activity. This changed the interfacial electronic structure and surface reactivity through the strong interaction and charge transfer between NiCo<sub>2</sub>S<sub>4</sub> and NiFe-LDH. And the calculated free energy of hydroxide chemisorption ( $\Delta E_{\text{OH}}$ ) decreases from 1.56 eV for pure NiFe-LDH to 1.03 eV for heterostructure, indicating a significant improvement in OER performance. Similarly, Gao et al. [31] prepared a simple heterostructure of nickel foam (Co<sub>9</sub>S<sub>8</sub>@NiFe-LDH/NF) with hollow Co<sub>9</sub>S<sub>8</sub> Nano arrays wrapped by NiFe layered double hydroxides as oxygen evolution reaction (OER) and hydrogen evolution reaction (HER) electrocatalyst to improve water-splitting efficiency. The preparation process is shown in Fig. 1, through structural design, strong electronic interactions were generated between each component to provide more active sites, higher charge transfer ability, and better electrochemical stability. In 1 M KOH solution, the overpotentials of Co<sub>9</sub>S<sub>8</sub>@NiFe-LDH/NF for OER and HER were 287 mV and 280 mV, respectively, resulting in a catalytic current density of 50 mA cm<sup>-2</sup>, and excellent HER and OER electrical properties are obtained.

In addition to transition metal sulfides and hydroxides, transition metal nitrides/carbides (TMNs/TMCs) also have a unique position in the field of water splitting due to their noble metal-like properties. Among them, TMCs presents a D-band structure similar to Pt through orbital hybridization, which brings high electrical conductivity and good mechanical strength, and shows excellent catalytic performance.

Leonard et al. [32] prepared four different phases of molybdenum carbide ( $\alpha$ -MoC<sub>1-x</sub>,  $\beta$ -Mo<sub>2</sub>C,  $\eta$ -MoC, and  $\gamma$ -MoC) and investigated their electrocatalytic activity for HER in an acidic

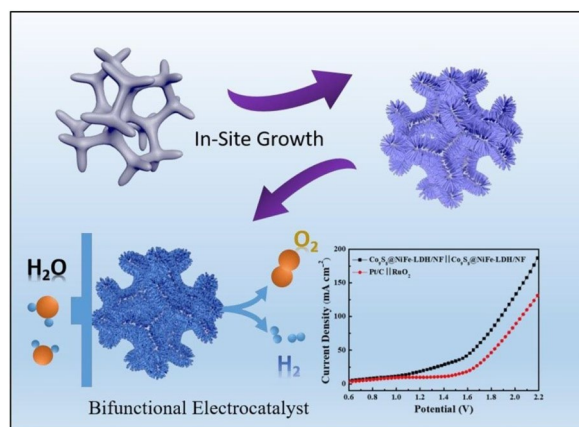
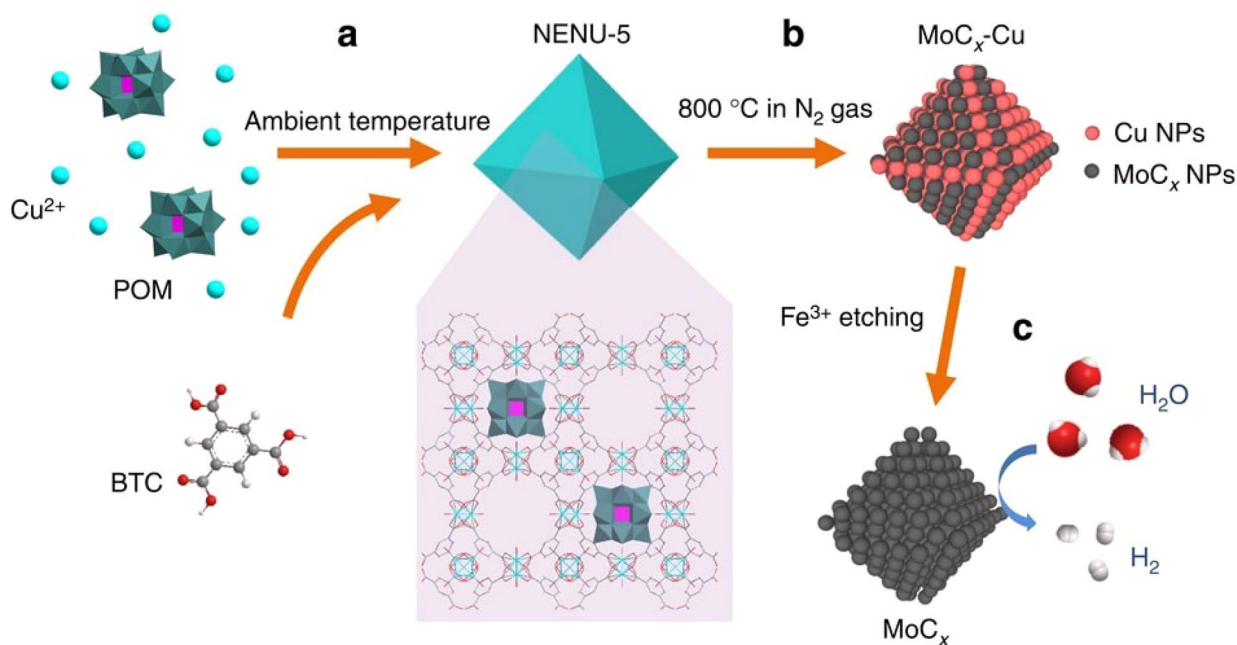


Figure 1: Preparation process of Co<sub>9</sub>S<sub>8</sub>@NiFe-LDH/NF [31].

solution.  $\beta$ -Mo<sub>2</sub>C was found to exhibit the highest electrocatalytic activity, while  $\gamma$ -MoC exhibited the second highest HER activity, and it exhibited excellent stability in acidic solutions. Traditional methods of synthesizing TMCs often require higher carburizing temperatures (> 700 °C), resulting in the sintering of TMC particles and a decrease in specific surface area. At the same time, TMC particles are also easily encapsulated by excess C precursors (such as CH<sub>4</sub> or CO), which will reduce the number of active sites of TMCs. However, Wu et al. [33] demonstrated a metal-organic framework-assisted strategy for the synthesis of nanostructured transition metal carbides based on confined carburization in a metal-organic framework matrix. As shown in Fig. 2, starting from a compound consisting of a Cu-based metal-organic framework host and a Mo-based polyoxometalate guest, mesoporous MoC<sub>x</sub> Nano-octahedrons composed of ultrafine nanocrystallites were successfully prepared, which exhibited remarkable hydrogen production performance from both acidic and alkaline solutions.

Compared with single-metal TMCs, constructing heterostructure is one of the effective ways to improve their catalytic activity [34]. Lin et al. [35] introduced electro spinning and pyrolysis to design Fe<sub>3</sub>C-Mo<sub>2</sub>C/nitrogen-doped carbon (Fe<sub>3</sub>C-Mo<sub>2</sub>C/NC) heterogeneous nanofibers (HNFs) with tunable compositions, resulting in abundant Fe<sub>3</sub>C-Mo<sub>2</sub>C heterogeneous interface to achieve synergy in electrocatalysis. Due to the strong hydrogen bonding on Mo<sub>2</sub>C and relatively weaker hydrogen bonding on Fe<sub>3</sub>C, the Fe<sub>3</sub>C-Mo<sub>2</sub>C interface significantly promotes HER kinetics and intrinsic activity. The final results showed that it only needed an overpotential of 116 mV and a Tafel slope of 43 mV dec<sup>-1</sup> at a current density of 10 mA cm<sup>-2</sup>, showing excellent water electrolysis performance. Yuan et al. [36] improved the electro catalytic performance of Mo<sub>2</sub>C by constructing a carbon-supported Co and Mo<sub>2</sub>C heterostructure (Co/Mo<sub>2</sub>C@C). Due to the synergistic effect between Co and Mo<sub>2</sub>C, electrons from Co could be transferred to Mo<sub>2</sub>C



**Figure 2:** (a) Synthesis of NENU-5 nano-octahedrons with Mo-based POMs residing in the pores of HKUST-1 host. (b) Formation of MoC<sub>x</sub>-Cu nano-octahedrons after annealing at 800 °C. (c) Removal of metallic Cu nanoparticles by Fe<sup>3+</sup> etching to produce porous MoC<sub>x</sub> nano-octahedrons for electrocatalytic hydrogen production [33].

and accumulated on Mo. This promoted the adsorption of OH<sup>-</sup> and desorption of H<sup>+</sup>, thereby enhancing the catalyst HER performance. Meanwhile, Co could inhibit the oxidation and dissolution of Mo<sub>2</sub>C through the “self-sacrifice” effect, which significantly improves the OER stability of Mo<sub>2</sub>C. Therefore, Co/Mo<sub>2</sub>C@C has a very good overall water-splitting performance.

Compared with a single metal, bimetallic TMCs have better corrosion resistance, and the bond strength between metal-H is also an important indicator for identifying electrocatalyst water splitting. If the metal-H bond strength is too weak, would cause the reactants to be difficult to adsorb, and if the metal-H bond strength is too strong, would cause the reactants to be difficult to desorb. Jaksic et al. demonstrated that the interaction between Ni and Mo can affect the HER via the hypothesized low-superd electron theory that is a synergistic effect is produced [37], so the appropriate metal-H bond strength is beneficial to the water-splitting process. Yu et al. [38] further tuned the electronic structure of Mo<sub>2</sub>C by element doping to enhance its electrocatalytic activity. The results showed that the electro catalytic activity sequence was as follows: Ni-Mo<sub>2</sub>C > Co-Mo<sub>2</sub>C > Fe-Mo<sub>2</sub>C > Cr-Mo<sub>2</sub>C. Therefore, Ni-Mo<sub>2</sub>C@C had the best HER performance, which showed overpotential of 72 mV at a current density of 10 mA cm<sup>-2</sup>, and a Tafel slope of 65.8 mV dec<sup>-1</sup>.

At the same time, TMC nanocomposites can prevent the aggregation of nanoparticles by combining with carbon materials (graphene, carbon nanotubes, etc.) to expose more active sites, and can be adjusted by the introduction of defects and impurity atoms (phosphorus, sulfur, etc.) to prove electron

transport ability, thereby improving the overall electro catalytic water-splitting ability of the composite [39, 40]. Lu et al. [41] rationally synthesized ultrafine carbides confined in Porous Nitrogen-doped Carbon Dodecahedrons (PNCs) by annealing a functional zeolite imidazole framework (ZIF-8) with molybdate or tungstate nanocrystals. By controlling the substitution amount of MO<sub>4</sub> units (M = Mo or W) in the ZIF-8 framework, biphasic carbide nanocrystals (denoted as MC-M<sub>2</sub>C/PNCs) confined in PNCs could be obtained. The uniformly distributed ultrafine nanocrystals facilitate the exposure of active sites and the PNCs acted as carriers to facilitate charge transfer and protected the nanocrystals from aggregation during HER. Furthermore, the strong coupling interaction between MC and M<sub>2</sub>C provided beneficial sites for water dissociation and hydrogen desorption. As a result, it exhibited better catalytic activity for HER than single-phase MC/PNC and M<sub>2</sub>C/PNC.

For TMNs, which are similar to TMCs, their cheap and efficient catalytic properties make them a potential substitute for noble metal water-splitting electrocatalyst. The preparation process of TMNs is similar to that of TMCs, which also uses NH<sub>3</sub> or N<sub>2</sub> to complete the nitriding operation. Among them, W-based nitrides are recognized as the most efficient electrocatalyst. Through a detailed study of the HER activity of atomically thin MoN nanosheets, Xie et al. [42] identified the active surface sites of atomically thin MoN nanosheets, where the surface Mo atoms could serve as active sites for converting protons to hydrogen. Similarly, TMNs can also greatly enhance the overall water-splitting performance of electrocatalyst by constructing

heterostructure. Diao et al. [34] developed a facile solid-state synthesis strategy to construct  $W_2N/WC$  heterostructure with abundant interfaces, benefiting from the synergy of the  $W_2N/WC$  interface to facilitate charge transport and separation, and accelerated the electrochemical ORR, OER, and HER, thereby exhibiting high efficiency overall water-splitting ability.

The theory of metal-H bond strength is also suitable for TMNs, so it is more beneficial to seek multi-metal TMNs to obtain medium-strength metal-H bonds. Cao et al. [43] obtained mixed close-packed  $Co_{0.6}Mo_{0.14}N_2$  particles by further treating  $Co_3Mo_3N$  with  $NH_3$  at low temperature through a two-step solid-state reaction for the preparation of cobalt-molybdenum nitrides with nanoscale morphology, which exhibited high catalytic activity and stability. Fan et al. [44] successfully prepared uniform  $Ni_3C$  Nano dots dispersed in ultrathin N-doped carbon nanosheets by carburizing a two-dimensional (2D) nickel cyanide coordination polymer precursor. Benefiting from a certain amount of Fe doping that optimized the electronic properties of  $Ni_3C$  and further improved the catalytic activity, N doping could adjust the electronic structure and was also beneficial to the electrocatalytic performance.

The construction of TMNs composites can also greatly improve the overall water-splitting performance of a single component. Guan et al. [45] improved the overall water-splitting ability of  $Ni_3N$  catalysts by utilizing  $FeOOH$  as a cocatalyst.  $FeOOH$  could promote the surface adsorption and crack of  $OH^-/H_2O$  species, which greatly reduced the d-band center of the active Ni species, thereby optimizing the Gibbs free energy of the intermediate. In addition, the relatively vertical  $Ni_3N$  nanotubes as the main catalyst can accelerate the mass and electron transfer, and the synergistic effect between the two could help to improve the HER/OER catalytic performance. Shu et al. [46] prepared  $Co_{5,47}N@N-rGO$  by a tannic acid-assisted nitridation method, benefiting from the unique worm-like structure to expose more active sites, and  $Co_{5,47}N$  nanoparticles with the synergistic advantage of the close contact between the N-rGO sheets, the nanocomposite exhibits highly efficient catalytic activity for both ORR and OER.

## TMNs for metal-air batteries

Metal-air batteries are one of the most efficient electrochemical energy storage devices among many types of energy storage and conversion. They have been widely studied due to their high efficiency, cleanliness, and low cost. The strong  $O=O$  bond ( $498 \text{ kJ}\cdot\text{mol}^{-1}$ ) needs to be broken during the electrochemical process, which is an important reason for the slow kinetics of the battery. Therefore, metal-air batteries usually require the help of additional catalysts. Currently, catalysts for ORR mainly include noble metal compounds, transition metal compounds, carbon-based materials, etc., among which the

high cost limits the development of precious metals in the field of air fuel cells.

On the contrast, transition metal compounds: Transition metals (such as Fe, Co, Ni, etc.) are abundant in the earth's crust, have abundant valence states, and can form various compounds. Given their abundant content, low cost, and tunable electronic structure, they are one of the popular electrocatalyst raw materials [47]. As the current research hotspot, transition metal compounds have been widely reported as efficient ORR catalysts and are expected to replace noble metal Pt/C [47]. However, the performance of a single transition metal compound is limited by electrical conductivity. Most of the materials with excellent performance are multi-component composites with C. For example, transition metal-nitrogen-carbon compounds have the advantages of simple synthesis, low price, and diverse compositions. It is the most excellent non-precious metal ORR catalyst at present, and its performance in acidic medium is close to that of noble metal, and even better than that of noble metal material in alkaline medium. Zhang et al. [48] successfully attached  $NiCo_2O_4$  nanowires to carbon cloth and made  $NiCo_2O_4/Zn$  batteries after preparing materials by hydrothermal method and annealing. Due to its independent nanostructure and oxygen defects, the annealed N- $NiCo_2O_4$  electrode exhibits good charge transfer rate, an initial capacity of  $169.5 \text{ mAh g}^{-1}$  at  $3.45 \text{ A g}^{-1}$  current density, and excellent cycle stability.

Transition metal hydroxides can also be used as efficient ORR and OER catalysts, but due to their poor stability, their structures need to be regulated to meet practical application needs. Li et al. [49] composited NiCo-LDH with various transition metal nanomaterials such as Fe and Ti and prepared a catalytic material with a large number of active sites, whose ORR half-wave potential ( $E_{1/2}$ ) was 80 mV, and after 33,000 s of ampere test, the current density decreased by only 5%, showing extremely high stability. The Zn-air batteries assembled with FePc-NiCo-LDH/ $Ti_3C_2$  air electrode exhibit a peak power density of  $148 \text{ mW}\cdot\text{cm}^{-2}$  and can be continuously charged and discharged for 80 h. Wang et al. [50] deposited 3–5-nm nickel-iron layered double hydroxide (NiFe-LDH) NiFe-LDH/Co, N-CNF on the surface of Co, N co-doped carbon nano frames (Co, N-CNF). The overpotential of the catalyst in the oxygen evolution reaction is 320 mV at a current density of  $10 \text{ mA cm}^{-2}$ , and the half-wave potential in the oxygen reduction reaction can reach 0.79 V. The excellent performance of the electrocatalyst was due to the high conductivity of Co,N-CNF and the strong NiFe-LDH interaction of 3–5 nm, which retained a large number of active sites.

Transition metal oxides have the advantages of abundant reserves, easy large-scale preparation, and low cost. Their ORR and OER properties can be modulated by various strategies, such as electronic structure modulation, defect engineering, and integration of appropriate carriers. The relationship between the

morphology and electrocatalytic performance of metal oxide-based catalysts has been extensively studied. In general, different exposed faces of a catalyst will exhibit significantly different physical and chemical properties. Zhang et al. [51] synthesized three different morphologies of cuprous oxide ( $\text{Cu}_2\text{O}$ ) (spherical, octahedral, and truncated octahedral) by potentiostatic electrodeposition. It is believed that the ORR activity of  $\text{Cu}_2\text{O}$  is significantly related to the morphology: among the three morphologies, the truncated octahedral  $\text{Cu}_2\text{O}$  has the highest ORR activity in alkaline media. DFT calculations show that  $\text{O}_2$  is more easily adsorbed on  $\text{Cu}_2\text{O}$  (100) (O–O bond length 1.43 Å), and the surface-adsorbed  $\text{O}_2$  on  $\text{Cu}_2\text{O}$  (100) is more easily activated than  $\text{Cu}_2\text{O}$ (111) (O–O bond length 1.37 Å) surface-adsorbed  $\text{O}_2$ . Engineering defects are also an effective way to tune the catalytic performance. He et al. [52] designed a CoO–S catalyst by introducing oxygen to occupy the oxygen vacancies on the surface of CoO, and O–Co–S enhanced the catalytic activity of CoO–S by a factor of 5 with a lower overpotential.

Transition metal phosphating is one of the few transition metal compounds with dual function catalysts of both ORR and OER, which has great potential in the field of rechargeable air battery. Li et al. [53] obtained  $\text{Ni}_{1.5}\text{Sn@triMPO}_4$  glass–ceramics by phosphating at low temperature, and then obtained novel glass–ceramics nanocrystal catalysts ( $\text{Ni}_{1.5}\text{Sn@triMPO}_4$ ) by hybridizing crystalline and amorphous tin-iron-nickel phosphate ( $\text{triMPO}_4$ ) through electrochemical activation, as shown in Fig. 3.

In the OER process, the crystal-amorphous structure reduces the vacancy formation energy of tin, indicating that this structure is more conducive to the precipitation of  $\text{Sn}^{4+}$ . At the same time, because the intrinsic oxygen vacancy generated by this structure has strong adsorption on  $\text{PO}_4^{3-}$ , the surface reconstruction is accelerated to form the actual catalytic center

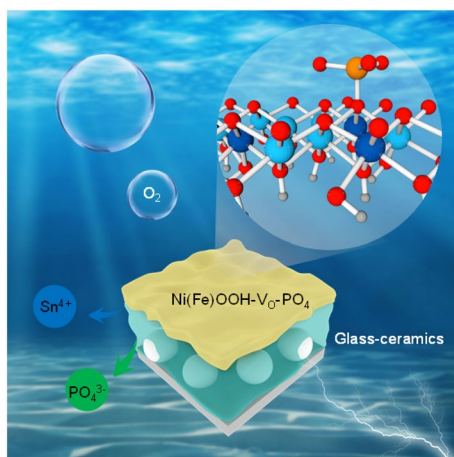


**Figure 3:** Glass–ceramics accelerates surface reconstruction and promotes OER reaction [53].

of  $\text{Ni(Fe)OOH-VO-PO}_4$ . The microcrystalline structure after surface reconstruction can enhance the OER process. Kang et al. [54] found that Fe dopant can effectively regulate the electronic conductivity of NiCoP and reduce the binding energy of reaction intermediates to the rate-determining steps of ORR and OER reactions. By implanting an amorphous carbon layer (Fe–NiCoP@C) catalyst on nickel foam, HSAB discharge voltage is 2.74 V at  $0.01 \text{ mA}\cdot\text{cm}^{-2}$  current density, and round-trip efficiency is 93.26% at the 500th cycle, showing good cycling performance.

Transition metal sulfides are widely used because of their suitable electronic band gaps, band locations, and exposed active sites. Ultrathin 2D metal sulfide nanostructures such as  $\text{MoS}_2$ ,  $\text{WS}_2$ , and  $\text{Co}_9\text{S}_8$  have a high surface area and excellent electron diffusion paths, thus showing interesting physical and chemical properties in energy conversion and storage studies. Exposed atoms on the surface increase the catalyst/electrolyte interface. Arunkumar et al. [55] increased the discharge capacity of magnesium metal-air battery from  $990 \text{ mAh}\cdot\text{g}^{-1}$  to  $1170 \text{ mAh}\cdot\text{g}^{-1}$  by adding  $\text{MoS}_2$  nanosheets into  $\text{MgCl}_2$  electrolyte. However, the pure transition metal sulfide with polycrystalline properties cannot fully develop its catalytic activity due to its poor electrical conductivity. Therefore, a great deal of effort has been put into researching new synthesis methods, including mixing or using highly conductive carrier materials. Carbon carriers, for example, have a high surface area, greater electronic conductivity, good mechanical properties, and excellent chemical stability, which greatly improves ORR/OER performance. Puglia et al. [56] used a simple stirring method to compound mechanically stripped  $\text{MoS}_2$  nanosheets with graphene, which showed strong redox activity in the cyclic voltammetry test. When  $\text{MoS}_2/\text{Gr} = 1:13$ , its catalytic activity was 25 times that of a single  $\text{MoS}_2$ , with an open-circuit voltage up to 1.4 V, and high specific energy of  $130 \text{ Wh}\cdot\text{kg}^{-1}$ . Hong et al. [57] prepared three different transition metal sulfide complexes using N–S-doped carbon matrix (i.e.,  $\text{MS@G/NSC}$ , where M: Fe, Co, Ni). Among them,  $\text{FeS@G/NSC}$  catalyst has high conductivity and high exposure activity region, has excellent ORR, its half-wave potential (E1/2) is about 0.88 V, and has excellent stability. Similarly, the N- and S-doped carbon-encapsulated  $\text{Co}_9\text{S}_8$  ( $\text{Co}_9\text{S}_8@\text{TDC-900}$ ) catalyst prepared by Zhao et al. [58] showed excellent electrocatalytic activity, E1/2 was about 0.78 V and only about 0.33 V overpotential at the current density of  $5.45 \text{ mA}\cdot\text{cm}^{-2}$ , with excellent cyclic stability.

### TMNs for supercapacitors

Electrode materials design is the subject of intense research in the field of energy development and advancement. Recently, transition metal-based nanomaterials (TMNs) have received great attention in supercapacitor application with regard to

excellent conductivity and outstanding physicochemical properties endowed by their inherent structures and unique chemical bonding. By preparing transition metal materials with different nanostructures, not only the advantages of low cost and good stability of transition metals can be used, but also the large surface area brought by the nanostructure of materials can be used to buffer the volume change of active materials. On this basis, the electrochemical energy storage performance can be further improved by compounding with other elements [59]. Therefore, it is necessary to methodically review the exploration and state-of-the-art modification of TMNs-based materials.

Feng et al. [60] reported a polymer intercalation method to synthesize three-dimensional MoS<sub>2</sub>/nitrogen-doped carbon composites. As shown in Fig. 4, after a series of processing, the MoS<sub>2</sub>/nitrogen-doped carbon material showed different interlayer spacing compared with pure MoS<sub>2</sub> nanosheets. The interlayer spacing of pure MoS<sub>2</sub> nanosheets after calcination was 0.62 nm, while that of MoS<sub>2</sub>/nitrogen-doped carbon composite was 0.98 nm. This value was consistent with the interlayer spacing of graphene embedded in MoS<sub>2</sub>, indicating that graphene was successfully embedded in the MoS<sub>2</sub> layer, which was caused by the in situ carbonization of PEI embedded in the MoS<sub>2</sub> layer. This electrode material had the following advantages: 1. The three-dimensional material structure was conducive to the fast transport of electrons and ions; 2. Since the graphene-like monolayer carbon was intercalated between the MoS<sub>2</sub> layers, MoS<sub>2</sub> exposed more accessible active sites for redox reactions and created new possibilities for ion/electron transport, which made each monolayer of MoS<sub>2</sub> electrochemically active; 3. The electrical conductivity of MoS<sub>2</sub> itself is very poor, but for the MoS<sub>2</sub>/nitrogen-doped carbon composites, electrons are transferred through metallic bond-like interfacial Mo–N bonds within the heterogeneous, which was more efficient than that through covalent bond-like Mo–O bonds within the MoS<sub>2</sub>/C hetero-aerogel. Therefore, MoS<sub>2</sub>/nitrogen-doped carbon material

exhibited excellent electrochemical performance, the mass specific capacitance was 4144 F g<sup>-1</sup> at a current density of 1 A g<sup>-1</sup>, and when the current density increased to 10 A g<sup>-1</sup>, the mass specific capacitance could still reach 2483 F g<sup>-1</sup>.

Compared with ordinary batteries, supercapacitors have higher power density, cycle efficiency, and energy density, and can perform up to millions of charge–discharge cycles. These properties offer great potential for the applications of stretchable supercapacitors in wearable and implantable energy devices. McPherson et al. [61] obtained a copper/copper oxide nanoporous electrode by selectively dissolving Al in Cu<sub>17.5</sub>Al<sub>82.5</sub> with NaOH, and formed a supercapacitor with an aqueous electrolyte. This device is safe and low cost, has very low ohmic losses, and can further increase the electrode surface area through geometric optimization. Zhou et al. [62] explored two-dimensional (2D) titanium carbide (Ti<sub>3</sub>C<sub>2</sub>T<sub>x</sub>) MXene for flexible and printed energy storage devices by fabrication of a robust, stretchable high-performance supercapacitor with reduced graphene oxide (RGO) to create a composite electrode. The Ti<sub>3</sub>C<sub>2</sub>T<sub>x</sub>/RGO composite electrode combined the excellent electrochemical and mechanical properties of Ti<sub>3</sub>C<sub>2</sub>T<sub>x</sub> with the mechanical robustness of RGO resulting from strong nanosheet interactions, larger nanoflake size, and mechanical flexibility. It was found that the Ti<sub>3</sub>C<sub>2</sub>T<sub>x</sub>/RGO composite electrodes with 50 wt% RGO incorporated proved to alleviate cracks generated under large strains. The composite electrodes exhibited a large capacitance of 49 mF cm<sup>-2</sup> (~ 490 F cm<sup>-3</sup> and ~ 140F g<sup>-1</sup>) and good electrochemical and mechanical stability when subjected to cyclic uniaxial (300%) or biaxial (200% × 200%) strains. The assembled symmetric supercapacitor had a specific capacitance of 18.6 mF cm<sup>-2</sup> (~ 90 F cm<sup>-3</sup> and ~ 29F g<sup>-1</sup>) and stretchability up to 300%. The developed method provided an alternative strategy to fabricate stretchable MXene-based energy storage devices and can be extended to other members of the large MXene family.

TMNs have been extensively studied for supercapacitor applications, but the synthesis of TMNs is a very difficult and

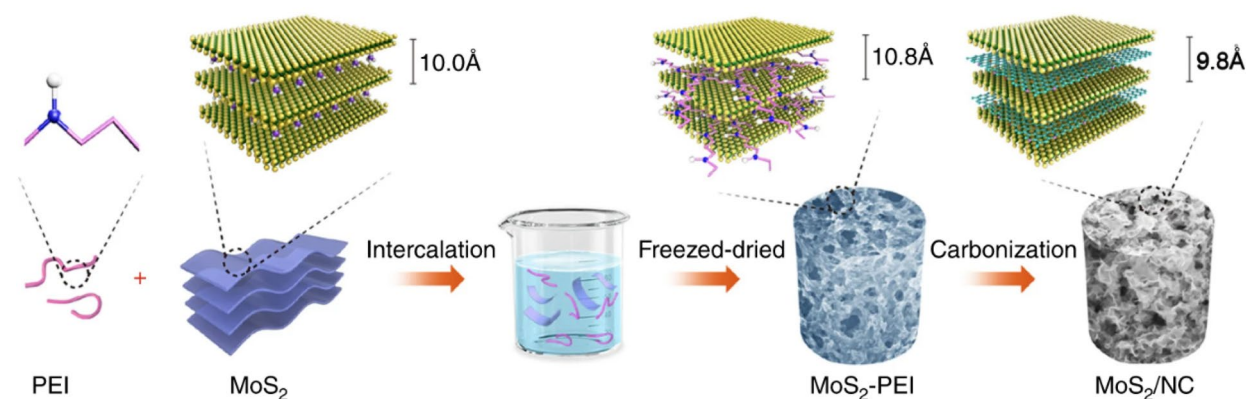


**Figure 4:** Synthesis of the MoS<sub>2</sub>/NC hetero-aerogel [60].

time-consuming process. TMOs and TMCs are promising electrode materials for next-generation ultracapacitors due to their multiple oxidation states. Therefore, it is a great challenge to enhance the electrochemical performance of pseudocapacitive materials by controlling their structure, morphology, and surface area. Hussain et al. [63] synthesized a binder-free zinc cobalt sulfide (ZCS)-based electrode via a facile single-step hydrothermal process. The obtained  $Zn_{0.76}Co_{0.24}S$  could be directly used as a binder-free electrode for supercapacitor applications. The effects of morphology on the electrochemical performance were also examined. Among the four electrodes, the synthesized 12-h ZCS had the highest specific capacitance of  $2417 \text{ F g}^{-1}$  ( $967 \text{ C g}^{-1}$ ) at  $1 \text{ A g}^{-1}$  and 83% good cycling stability after 10,000 charge/discharge cycles. Furthermore, an asymmetric supercapacitor (ASC) with  $Zn_{0.76}Co_{0.24}S$  as the positive electrode and activated carbon (AC) as the negative electrode exhibited a high energy density of  $51 \text{ W h kg}^{-1}$  at a power density of  $400 \text{ W kg}^{-1}$  and good cycling stability of 82% after 5000 cycles.

Among the metal sulfides candidates, manganese sulfide (MnS) exhibits interesting properties, such as low cost, excellent electrochemical performance, environmental friendliness, and natural abundance. This is the most promising electrode material for next-generation supercapacitors because of its theoretical SC as high as  $1370 \text{ F g}^{-1}$  in aqueous electrolytes. Compared with ternary transition metal oxides, transition metal sulfides generally exhibit higher conductivity, ionic diffusivity due to substitution of oxygen by sulfur atoms, narrow band-gap, large anionic polarizability, and larger size of the  $S^{2-}$  ion. Rao et al. [64] reported the facile synthesis of a novel Cu-MnS structure with PVP, in which the complementary features of the high theoretical capacitance of MnS, low cost, and high electrical conductivity of Cu as well as the appreciable surface area with the high thermal and mechanical conductivity of PVP, fabricating high-performance electrodes for supercapacitor applications on a single entity on nickel foam. The active phases of Cu and PVP in MnS promoted ion diffusion at the interfaces, and the void space between particles can withstand volume changes during long-term cycling. The electrochemical tests showed the as-prepared Cu-MnS with the 2PVP electrode exhibited an extraordinary SC of  $833.58 \text{ F g}^{-1}$  at a current density of  $1 \text{ A g}^{-1}$  and a very high cycling stability of 96.95% over 1000 cycles in  $2 \text{ M KOH}$  solution. Therefore, it may provide a new route for the commercialization of transition metal-based nanomaterial supercapacitors.

Molybdenum disulfide ( $MoS_2$ ), a class of TMDCs, is one of the most studied materials due to its advantages: excellent electrocatalytic activity, 2D layered crystal structure that facilitates ion intercalation, high surface area, and higher electronic conductivity than transition metal oxides (TMOs). It was not until 2007, when the capacitive behavior of  $MoS_2$  nanowall films was first reported, that researchers

considered using TMDC for supercapacitors. Balasingam et al. [65] adopted the facile hydrothermal method to deposit an amorphous  $MoS_x$  thin layer on the carbon fiber paper. The as-synthesized binder-free electrode material exhibited excellent electrochemical energy storage capacity and symmetric device with a high specific device capacitance value of  $41.96 \text{ mF cm}^{-2}$ . The capacitance retention of amorphous  $MoS_x$  increased up to 600% in the presence of a sulfuric acid medium due to “electro-activation.” Li et al. [66] prepared an advanced electrode of supercapacitor by electrochemically depositing  $MoS_2$  into TiN nanotube arrays (NTAs) on a Ti mesh substrate. The sample with 900 pulses had the highest specific capacitance of  $353.2 \text{ F/g}$  at  $0.6 \text{ A/g}$  and the lowest internal resistance of  $2.195 \Omega$  and interface resistance of  $0.005 \Omega$ . The specific capacitance retention was 63% after 700 galvanostatic charge/discharge cycles at a current density of  $0.8 \text{ A/g}$ . Combined good conductivity of TiN nanotubes and high theoretical specific capacitance of  $MoS_2$  nanoparticles, the hybrid electrode was expected to provide high electrochemical performance for supercapacitors.

The most common phase of  $MoS_2$  is 2H because of its stability; however, it is not ideal for energy storage applications due to its semiconducting properties. The electrical conductivity of metallic phase 1T- $MoS_2$  is 107 times higher than that of 2H- $MoS_2$ , making it a new favorite in the field of energy storage and has recently been used in batteries and supercapacitors. Zhuo et al. [67] combined the benefits of aryl diazonium functionalized graphene (“fct-graphene”) with chemically exfoliated 1T- $MoS_2$  to produce composite fct-graphene/1T- $MoS_2$  electrodes, as shown in Fig. 5. The typically metastable 1T- $MoS_2$  was stabilized by the interaction with fct-graphene, preventing it from reverting to the 2H phase. The alternative layer graphene- $MoS_2$  structure led to a high specific capacitance ( $290 \text{ F cm}^{-3}$  at  $0.5 \text{ A g}^{-1}$ ) and 90% capacitance retention after 10,000 cycles. These beneficial electrochemical properties were attributed to hydrophilicity, high electronic conductivity, enlarged interlayer space, and shortened ion diffusion length, which demonstrated the potential to develop high-performance energy storage.

Among the various pseudocapacitive transition metal oxides studied for supercapacitors,  $MnO_2$  is favored due to its low cost, low toxicity, natural abundance, high theoretical pseudo capacitance (about  $1370 \text{ F g}^{-1}$ ), and friendly interfacial properties with carbon materials. Among the different phases of  $MnO_2$ , the  $\epsilon$ -phase is known for its electrochemical activity. Rakhi et al. [68] fabricated symmetric supercapacitors using  $\epsilon$ - $MnO_2/Ti_2CT_x$  and  $\epsilon$ - $MnO_2/Ti_3C_2T_x$  composites. Combined with the enhanced pseudo capacitance, the  $\epsilon$ - $MnO_2/MXene$  supercapacitor exhibited excellent cycling stability, retaining about 88% of the initial specific capacitance retained after 10,000 cycles. The proposed electrode structure



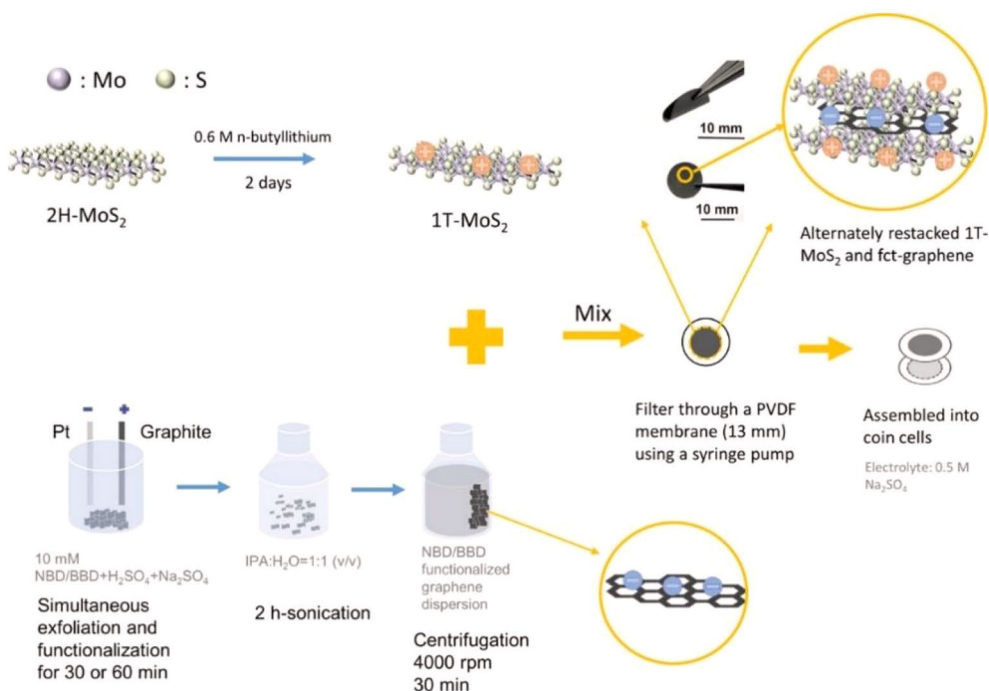


**Figure 5:** Schematic showing the 1T-MoS<sub>2</sub>/ fct-graphene composite production procedure [67].

took advantage of the high specific capacitance of MnO<sub>2</sub> and the ability of MXenes to improve conductivity and cycling stability.

### TMNs for fuel cells

Fuel cells use oxygen as an oxidant to convert chemical energy stored in biomass fuel into electricity. The electrochemical reactions in fuel cells consist of anodic fuel oxidation and cathodic oxygen reduction reaction (ORR). The slow reaction kinetics of cathode reaction is the main factor restricting the wide commercial application of fuel cell. Platinum and its alloys have proved to be the most dynamic ORR electrocatalysts [69, 70]. But platinum is not only expensive, scarce, and nondurable. In addition, as a catalyst for fuel cells, platinum also has the disadvantage of easy poisoning. Therefore, a great deal of research has focused on exploring new catalysts with low cost and high performance. Transition metal compounds (e.g., oxides, nitrides, carbides, hydroxides, sulfides) can be used as promising electrocatalysts to replace platinum [71–73].

Transition metal nitrides have attracted much attention due to their unique electronic structure, high electrical conductivity, high hardness, high density, and corrosion resistance. Varga et al. [74] synthesized nitrogen-doped graphene sheets modified with cobalt nitride (Co<sub>4</sub>N) nanoparticles from freeze-dried GO nanosheets and cobalt acetate (II) in an ammonia atmosphere of 600 °C. With the increase of cobalt content, the average particle size of Co<sub>4</sub>N increases from 14 to 201 nm. The oxygen reduction

activity of the new catalyst is comparable to that of the widely used Pt/C. Under alkaline conditions, the reduction current density is the highest, up to 4.1 mA cm<sup>-2</sup>. Rui et al. [75] prepared a series of carbon-supported metal nitrides (M<sub>x</sub>N / C, M = Ti, V, Cr, Mn, Fe, Co, Ni, x = 1 or 3) by nitriding with ammonia. The introduction of carbon carrier promotes the dispersion of transition metal nitrides, thus maximizing the utilization rate of nitrogen compounds. And when the material is exposed to air, it forms a thin shell of oxygen-based oxides that provides a surface for catalyzing chemical reactions. Electrochemical measurements in alkaline electrolytes show that Co<sub>3</sub>N/C, MnN/C, and Fe<sub>3</sub>N/C show good ORR activities, with Co<sub>3</sub>N/C exhibiting the highest ORR performance, which is comparable to commercial Pt/C. When Co<sub>3</sub>N/C was used as the cathode catalyst for anion exchange membrane fuel cells (AEMFCs) in anion exchange membrane fuel cells, its peak power density (PPD) reached 700 mW cm<sup>-2</sup>, which represented the highest membrane electrode assemblies (MEAs) among the reported nitride cathode catalysts performance.

Transition metal oxides have the characteristics of low cost, high activity, and environmental protection, and are reliable cathode catalyst materials for fuel cells. Among them, Mn- and Co-based oxides have the best ORR catalytic activity. Manganese oxides have received extensive attention due to their remarkable advantages such as low cost, environmental friendliness, multivalent state, and abundant crystal structure [76]. The results show that the ORR catalytic activity of Mn oxide

catalysts with different valence states increases with the increase of Mn valence state, and the ORR catalytic activity of Mn oxide catalysts obtained at high potential is significantly higher than that obtained at low potential. Zhang et al. [77] prepared manganese defect  $\text{Mn}_3\text{O}_4$  by calcination of manganese glycerate. Experimental and calculated results show that the Mn defect in  $\text{Mn}_3\text{O}_4$  changes the electronic structure, improves the electrical conductivity and electron delocalization, and contributes to the exposure of more surface  $\text{Mn}^{3+}$  as the main active site, thus promoting the activation of  $\text{O}_2$  and the desorption of  $\text{OH}^*$ , and effectively reducing the limiting rate Gibbs free energy and theoretical overpotential change of the material. The onset potential, half-wave potential, and limiting current density of  $\text{Mn}_3\text{O}_4$  with Mn defects are 0.87 V, 0.65 V, and  $5.0 \text{ mA}\cdot\text{cm}^{-2}$ , respectively, which are better than those of ordinary  $\text{Mn}_3\text{O}_4$  (0.77 V, 0.62 V, and  $2.6 \text{ mA}\cdot\text{cm}^{-2}$ ).

Cobalt oxide has attracted a lot of interest because of its good performance, low cost, and high stability. Ma et al. [78] used Ar plasma etching technology to prepare cobalt oxide rich in oxygen vacancies (expressed as  $\text{Co}_3\text{O}_{4-x}$ ), and thus prepared a new type of zinc-cobalt oxide and zinc-air hybrid battery.  $\text{Co}_3\text{O}_{4-x}$  can successfully perform a number of electrochemical reactions, including ORR/ OER electrocatalytic reaction and faraday  $\text{Co}-\text{O} \leftrightarrow \text{Co}-\text{O}-\text{OH}$  redox reaction. The novel hybrid zinc-based power cell not only has a high-power density of  $3200 \text{ W}\cdot\text{kg}^{-1}$ , but also has a high energy density of  $1060 \text{ Wh}\cdot\text{kg}^{-1}$ , and still has good electrochemical stability after 1500 cycles of 440 h. More importantly, the solid-state hybrid battery also demonstrated good safety, excellent water resistance, and washable ability after being immersed in water for 20 h or washed for 1 h, maintaining electrochemical performance of nearly 90% or more. In addition, the new hybrid zinc-based power battery can automatically restore power output when exposed to air.

Transition metal carbides are cheap and readily available materials, which have good electrical conductivity and special electronic structure, and are potential electrocatalysts to replace precious metals. Xiao et al. [79] polymerized 1,8-diaminonaphthalene with ferric chloride, and obtained a porous nitrogen-doped carbon material encapsulating  $\text{Fe}_3\text{C}$  nanoparticles in a graphite layer by pyrolysis and etching. Among them, the sample  $\text{Fe}_3\text{C}/\text{NG}-800$  at  $800^\circ\text{C}$  has the largest specific surface area, and materials with high specific surface area can provide more active sites; at the same time, appropriate pore structure and distribution can accelerate the mass transfer rate and improve the catalytic efficiency. The onset potential and half-wave potential of  $\text{Fe}_3\text{C}/\text{NG}-800$  in  $0.1 \text{ mol/L HClO}_4$  solution were 0.92 V and 0.77 V, respectively, and the resistance to methanol and carbon monoxide of  $\text{Fe}_3\text{C}/\text{NG}-800$  was much higher than that of commercial platinum carbon. In  $0.1 \text{ mol/L KOH}$  solution, the onset potential and half-wave potential of  $\text{Fe}_3\text{C}/\text{NG}-800$  are 1.03 V

and 0.86 V, respectively, even higher than that of commercial platinum carbon, and its stability is also higher than that of commercial platinum carbon. In addition, WC has excellent catalytic performance due to its properties of covalent compounds, ionic crystals, and transition metal materials. WC has good acid resistance and catalytic activity for the electro-oxidation of methanol. However, WC prepared by high temperature carbonization is easy to be covered by elemental carbon on the surface of the catalytic active site, which reduces its catalytic activity. So, WC catalysis before use, the agent needs to remove the carbon covered on the surface, exposing the catalyst activity site, so that the maximum catalytic activity is shown. Weigert et al. [80] prepared WC and Pt-modified WC as anode catalysts for DMFC, and evaluated their catalytic activity and stability. The results of temperature step-up desorption and high-resolution electron energy loss spectroscopy show that WC is more active to dissociate methanol and water than Pt and Ru. The desorption temperature of WC for CO is at least 100 K lower than that of Pt and Ru. WC has a higher tolerance to CO poisoning in the electro-oxidation process of catalytic methanol. Sheng et al. [81] prepared a series of Pt-modified WC catalysts. DFT calculation results showed that double-layer Pt-modified WC and Pt (111) catalyst had similar methanol electro-oxidation initial potential, and its reaction activity was 2.4 times higher than that of pure Pt. The synergistic effect of Pt and WC also provides a new carrier for anodic catalyst.

### TMNs for lithium-ion batteries

With the popularity of electric vehicles (EV) in recent years, the market demand for lithium-ion batteries is growing rapidly. At present, the main commercial anode material graphite is limited by low theoretical capacity and low lithium-ion transfer rate, which seriously limits the storage performance of lithium-ion batteries [82–84]. Therefore, the research and application of new anode materials are very important. Transition metal-based nanomaterials have high theoretical capacity, and they have excellent cycle performance and Coulomb efficiency through the preparation of special morphologies or composites, and become competitive candidates for next-generation anode materials.

There are three different lithium-ion storage mechanisms (I) insertion, (II) alloying, and (III) transformation when transition metal oxides are used as anode active materials. In the first insertion type, titanium is mainly the active center, which is reduced to positive trivalent titanium during lithium implantation and oxidized to positive tetra valent titanium when lithium ions are detached. The material using this mechanism has a very small volume change during charge and discharge, maintaining the integrity of the structure and excellent cycling performance. Lithium ions are stored reversibly in the active material, but the deficiency lies in its very high molar mass and low theoretical specific capacity

[85]. The second alloying material, which is the opposite of the insert material, has a very high theoretical specific capacity and is reduced to metallic elements during the cycle. However, when the active surface contact with electrolyte, it will lead to electrolyte decomposition and solid electrolyte interface formation, and in the process of charging and discharging, volume expansion is serious, resulting in poor stability. In view of the characteristics of the two transition metal oxides, researchers focused on the study of nanostructures to improve their shortcomings.

Luo et al. [86] reported a method of successfully grafting continuous mesoporous nanostructure  $\text{Fe}_3\text{O}_4$  onto 3D graphene foams assisted by atomic layer deposition. The loose and porous structure of graphene alleviates the problem of shedding or pulverization of active materials caused by volume expansion. The composite material is directly used as the negative electrode of lithium-ion batteries, with high reversible capacity and rapid discharge capability. The capacity is up to  $785\text{mAh g}^{-1}$  at 1C and remains stable in 500 charge and discharge cycles. Larson et al. [87] successfully prepared nanoporous molybdenum oxide asymmetric membranes through spontaneous non-solvent-induced phase separation. The three-dimensional nanoporous structure can alleviate the large volume change during charging and discharging, and effectively increase the cycle stability of lithium-ion battery anodes. The experimental results also prove that the lithium-ion battery composed of the  $\text{MoO}_2$  plane asymmetric film anode material can still maintain 97% of the initial capacity after 165 cycles at a current density of  $120\text{mAh g}^{-1}$ . At present, mixed transition metal oxides are also studied. Compared with common metal oxides, the two metal elements have different expansion coefficients, resulting in a synergistic effect to buffer volume expansion. Moreover, both elements are electrochemically active metals, which can form alloys with more lithium ions and have better electrochemical performance. Liu et al. [88] synthesized a hierarchical 3D  $\text{ZnCo}_2\text{O}_4$  nanowire array/carbon cloth composite as a non-viscous negative electrode of lithium ion, as shown in Fig. 6, the reversible capacity reached  $1300\text{--}1400\text{mAh g}^{-1}$ , and after 160 cycles, its capacity is still  $1200\text{mAh g}^{-1}$ . Recently, Yu et al. [89] reported a method to synthesize a series of  $\text{Li}_{1-2}\text{Ni}_{0.3}\text{Ti}_{0.3}\text{Nb}_{0.2}\text{O}_2$  (LNTNO20)@C using different mass ratios of carbon precursors and calcination temperatures, proposing the use of a carbon coating process to increase the height of the tetrahedron makes the diffusion of lithium ions easier, and hinders the reaction between the active material and the electrolyte, reduces the polarization during cycling, and exhibits excellent cycling stability.

Compared with transition metal oxides, metal sulfides have better prospects in the field of anode materials due to their smaller volume expansion. At present, there are researches on large-scale synthesis of high-quality 2D 1 T-phase  $\text{MoS}_2$ , which is expected to be widely used in lithium-ion batteries [90, 91]. Most metal sulfides hold lithium ions at voltages less than 1.5 V

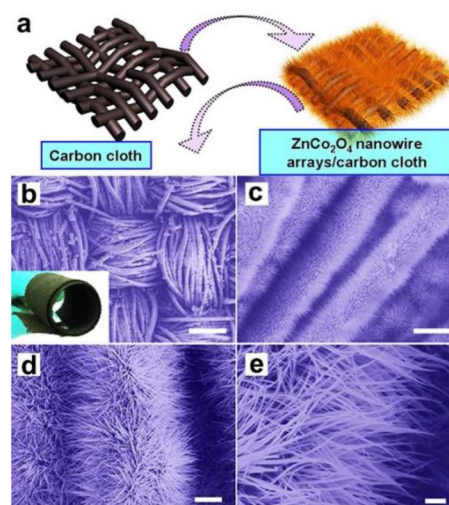


**Figure 6:** (a) Schematic illustration of the synthesis of flexible 3D  $\text{ZnCo}_2\text{O}_4$  nanowire arrays/carbon cloth. Morphology characterization. (b–e) Typical FESEM images of the  $\text{ZnCo}_2\text{O}_4$  nanowire arrays growing on carbon cloth at different magnifications. Scale bars,  $200\ \mu\text{m}$  (b);  $20\ \mu\text{m}$  (c);  $5\ \mu\text{m}$  (d);  $1\ \mu\text{m}$  (e) [88].

vs.  $\text{Li}/\text{Li}^+$ , a reaction mechanism that allows for higher energy densities. However, during the first charge and discharge, the electrode material tends to crack the active material due to volume expansion, which in turn leads to a rapid decay of the specific capacity, and the Coulombic efficiency is particularly low. At present, researchers mainly improve the cycle stability of batteries by compounding with other structurally stable and conductive materials, such as graphene and carbon nanotubes, or preparing special layered transition metal sulfides to alleviate the strain in the conversion reaction. Kalimuldina et al. [92] employed spray pyrolysis and subsequent thermal treatment to prepare  $\text{Cu}_2\text{S}$  with a monoclinic crystal structure of space group  $\text{P}2_1/\text{C}$ . After the material was coated on carbon brazing paper, the reversible stable capacity was  $330\text{mAh g}^{-1}$  after 20 cycles at 0.1C current density, which was close to 98% of its theoretical capacity. By increasing the discharge cut-off voltage, the capacity is gradually reduced to avoid the formation of a solid electrolyte interface during the first cycle. Xiao et al. [93] reported a strategy for the preparation of carbon-free  $\text{CoS}_x$  with hollow structures by simple solvothermal reaction and annealing. This unique nanostructure has a hollow core and a porous shell, which is comparable to the solid structure in which both rate capability and cycling stability have been improved. For example, its initial discharge capacity is as high as  $1059.7\text{mAh g}^{-1}$ , the Coulombic efficiency reaches 77.2%, and the reversible capacity reaches  $1012.1\text{mAh g}^{-1}$  after 100 cycles at a current of  $500\text{mA g}^{-1}$ . Fayed et al. [94] prepared nitrogen and carbon co-doped molybdenum disulfide nanosheets by a one-step method.  $\text{MoS}_2$  samples promote the diffusion of ions through disordered nanosheet-like aggregates, thereby enhancing the

electrochemical performance. For lithium-ion batteries, the material achieves a first discharge capacity of  $1280 \text{ mAh g}^{-1}$  at a current density of  $100 \text{ mA g}^{-1}$ , and the rate performance is not bad.

For other transition metal nanomaterials, due to the low conversion reaction sites between transition metal nitrides and Li, metal nitrides have better performance in lithium-ion anode materials. Lai et al. [95] reported a general method for the synthesis of transition metal nitride nanoparticles by anchoring the nanoparticles on conductive graphene as anode materials for Li-ion batteries. This method is suitable for anchoring FeN, FeCoN, CoN, NiN, etc. on conductive N-modified graphene. This hybrid material has high specific capacity and good cycle performance. Even if the loading is reduced, it can improve the lithium-ion storage capacity of graphene. For example, when the nanoparticles are FeN, the initial reversible capacity of the hybrid material is about  $665 \text{ mAh g}^{-1}$  at a current density of  $50 \text{ mA g}^{-1}$ , and the capacity will continue to rise to  $698 \text{ mAh g}^{-1}$  in the subsequent cycling process, showing good cycle performance. Wang et al. [96] used two-dimensional titanium carbide (MXene) metal conductive film as the current collector layer of the electrode material, and multilayer  $\text{Ti}_3\text{C}_2\text{T}_x$  ( $\text{T}_x$  is the surface functional group) as the negative electrode material. The study found that the  $\text{Ti}_3\text{C}_2\text{T}_x$  MXene current collector reduces the weight and thickness of the device without changing the performance. This study extends the application of transition metal carbides in Li-ion batteries as current collectors without additional surface treatment and may be an effective candidate for the development of flexible and lightweight energy storage devices.

## Acknowledgments

The authors wish to thank the facility support of the Center for Nanoscale Characterization & Devices, WNLO of Huazhong University of Science and Technology (HUST), the Analytical and Testing Center of HUST, and the financial support from Knowledge Innovation Program of Wuhan-Basic Research (2022010801010352).

## Data availability

The datasets generated during and/or analyzed during the current study are available from the corresponding author on reasonable request.

## Code availability

Not applicable.

## Declarations

**Conflict of interest** On behalf of all authors, the corresponding author states that there is no conflict of interest.

## References

1. A.G. Olabi, M. Mahmoud, B. Soudan et al., Geothermal based hybrid energy systems, toward eco-friendly energy approaches. *Renew. Energy*. **147**, 2003 (2020)
2. R. Qin, P. Wang, C. Lin et al., Transition metal nitrides: Activity origin, synthesis and electrocatalytic applications. *Acta Phys.-Chim. Sin.* **37**, 2009099 (2020)
3. J. Zheng, W. Zhang, J. Zhang et al., Recent advances in nanostructured transition metal nitrides for fuel cells. *J. Mater. Chem. A*. **8**, 20803 (2020)
4. L. Lin, S. Piao, Y. Choi et al., Nanostructured transition metal nitrides as emerging electrocatalysts for water electrolysis: Status and challenges. *Energy Chem.* **4**, 100072 (2022)
5. E. Hu, Y. Feng, J. Nai et al., Construction of hierarchical Ni-Co-P hollow nanobricks with oriented nanosheets for efficient overall water splitting. *Energy Environ. Sci.* **11**, 872 (2018)
6. D.H. Youn, G. Bae, S. Han et al., A highly efficient transition metal nitride-based electrocatalyst for oxygen reduction reaction: TiN on a CNT-graphene hybrid support. *J. Mater. Chem. A*. **1**, 2007 (2013)
7. Y. Men, P. Li, F. Yang et al., Nitrogen-doped CoP as robust electrocatalyst for high-efficiency pH-universal hydrogen evolution reaction. *Appl. Catal. B-Environ.* **253**, 21 (2019)
8. X. Dong, H. Yan, Y. Jiao et al., 3D hierarchical V-Ni-based nitride heterostructure as a highly efficient pH-universal electrocatalyst for the hydrogen evolution reaction. *J. Mater. Chem. A*. **7**, 15823 (2019)
9. Y. Yuan, J. Wang, S. Adimi et al., Zirconium nitride catalysts surpass platinum for oxygen reduction. *Nat. Mater.* **19**, 282 (2020)
10. Y. Han, X. Yue, Y. Jin et al., Hydrogen evolution reaction in acidic media on single-crystalline titanium nitride nanowires as an efficient non-noble metal electrocatalyst. *J. Mater. Chem. A*. **4**, 3673 (2016)
11. Z. Fu, N. Wang, D. Legut et al., Rational design of flexible two-dimensional MXenes with multiple functionalities. *Chem. Rev.* **119**, 11980 (2019)
12. Z. Wang, V. Kochat, P. Pandey et al., Metal immiscibility route to synthesis of ultrathin carbides, borides, and nitrides. *Adv. Mater.* **29**, 1700364 (2017)
13. H. Jin, Q. Gu, B. Chen et al., Molten salt-directed catalytic synthesis of 2D layered transition-metal nitrides for efficient hydrogen evolution. *Chem.* **6**, 2382 (2020)
14. Y. Wu, J. Wu, L. Jiao et al., Cascade reaction system integrating single-atom nanozymes with abundant Cu sites for enhanced biosensing. *Anal. Chem.* **92**, 3373 (2020)

15. Y. Luo, H. Jin, Y. Lu et al., Potential gradient-driven fast-switching electrochromic device. *ACS Energy Lett.* **7**, 1880 (2022)
16. L. Jiao, J. Wu, H. Zhong et al., Densely isolated FeN<sub>4</sub> sites for peroxidase mimicking. *ACS Catal.* **10**, 6422 (2020)
17. K. Liu, H. Jin, L. Huang et al., Puffing ultrathin oxides with non-layered structures. *Sci. Adv.* **8**, 2030 (2022)
18. Q. Li, J. Wu, T. Wu et al., Phase engineering of atomically thin perovskite oxide for highly active oxygen evolution. *Adv. Funct. Mater.* **31**, 2102002 (2021)
19. Y. Li, J. Wu, B. Zhang et al., Fast conversion and controlled deposition of lithium (poly)sulfides in lithium-sulfur batteries using high-loading cobalt single atoms. *Energy Storage Mater.* **30**, 250 (2020)
20. H. Jin, F. Li, J. Gao et al., Additive-free ultrastable hydrated Vanadium Oxide Sol/Carbon nanotube ink for durable and high-power aqueous zinc-ion battery. *Adv. Mater. Interfaces.* **9**, 2200174 (2022)
21. G. Zhang, T. Wu, H. Zhou et al., Rich Alkali Ions preintercalated vanadium oxides for durable and fast zinc-ion storage. *ACS Energy Lett.* **6**, 2111 (2021)
22. Y.H. Guo, L. Zhao, D.Y. Zheng, Theoretical investigation on the electronic structure of new InSe/CrS<sub>2</sub> van der Waals heterostructure. *J. Mater. Res.* (2022). <https://doi.org/10.1557/s43578-022-00548-8>
23. P. Foroughi, A. Durygin, S.C. Sun et al., Flash sintering of tantalum-hafnium diboride solid solution powder. *J. Mater. Res.* (2022). <https://doi.org/10.1557/s43578-022-00492-7>
24. Q. Sun, J. Liu, Y. Xie et al., Monodisperse MnO Nanoparticles in situ Grown on Reduced Graphene Oxide via hydrophobic interaction for Excellent Electromagnetic Wave Absorption. *J. Mater. Res.* (2022). <https://doi.org/10.1557/s43578-022-00491-8>
25. S. Xiong, D. Liang, Effect of sol process on structure and luminescent properties of nano-Mn<sub>3</sub>B<sub>7</sub>O<sub>13</sub>Cl. *J. Mater. Res.* (2022). <https://doi.org/10.1557/s43578-022-00499-0>
26. Yu.S. Yapontseva, T.V. Maltseva, V.S. Kublanovsky et al., Electrodeposition and properties of CoWRe alloys. *J. Mater. Res.* (2022). <https://doi.org/10.1557/s43578-022-00497-2>
27. G. Zhao, K. Rui, S.X. Dou et al., Boosting electrochemical water oxidation: the merits of heterostructured electrocatalysts. *J. Mater. Chem. A.* **8**, 6393 (2020)
28. B. Song, S. Jin, Two are better than one: Heterostructures improve hydrogen evolution catalysis. *Joule.* **1**, 220 (2017)
29. P. Xiong, X. Zhang, H. Wan et al., Interface modulation of two-dimensional superlattices for efficient overall water splitting. *Nano Lett.* **19**, 4518 (2019)
30. J. Liu, J. Wang, B. Zhang et al., Hierarchical NiCo<sub>2</sub>S<sub>4</sub>@NiFe LDH heterostructures supported on nickel foam for enhanced overall-water-splitting activity. *ACS Appl. Mater. Inter.* **9**, 15364 (2017)
31. X.T. Gao, Z. Yu, K.X. Zheng et al., Hollow Co<sub>9</sub>S<sub>8</sub>@NiFe-LDH nanoarrays supported by nickel foam for boosting the overall water-splitting performance. *Mater. Lett.* **319**, 132302 (2022)
32. C. Wan, Y.N. Regmi, B.M. Leonard, Multiple phases of molybdenum carbide as electrocatalysts for the hydrogen evolution reaction. *Angew. Chem. Int. Ed.* **53**, 6407 (2014)
33. H.B. Wu, B.Y. Xia, L. Yu et al., Porous molybdenum carbide nano-octahedrons synthesized via confined carburization in metal-organic frameworks for efficient hydrogen production. *Nat. Commun.* **6**, 6512 (2015)
34. J. Diao, Y. Qiu, S. Liu et al., Interfacial engineering of W<sub>2</sub>N/WC heterostructures derived from solid-state synthesis: A highly efficient trifunctional electrocatalyst for ORR, OER, and HER. *Adv. Mater.* **32**, 1905679 (2020)
35. H. Lin, W. Zhang, Z. Shi et al., Electrospinning heteronanofibers of Fe<sub>3</sub>C-Mo<sub>2</sub>C/Nitrogen-Doped-Carbon as efficient electrocatalysts for hydrogen evolution. *Chemsuschem* **10**, 2597 (2017)
36. S. Yuan, M. Xia, Z. Liu et al., Dual synergistic effects between Co and Mo<sub>2</sub>C in Co/Mo<sub>2</sub>C heterostructure for electrocatalytic overall water splitting. *Chem. Eng. J.* **430**, 132697 (2022)
37. M.M. Jakšić, Hypo-hyper-d-electronic interactive nature of synergism in catalysis and electrocatalysis for hydrogen reactions. *Electrochim. Acta.* **45**, 4085 (2000)
38. F. Yu, Y. Gao, Z. Lang et al., Electrocatalytic performance of ultrasmall Mo<sub>2</sub>C affected by different transition metal dopants in hydrogen evolution reaction. *Nanoscale* **10**, 6080 (2018)
39. Y.Y. Chen, Y. Zhang, W.J. Jiang et al., Pomegranate-like N, P-Doped Mo<sub>2</sub>C@C nanospheres as highly active electrocatalysts for alkaline hydrogen evolution. *ACS Nano* **10**, 8851 (2016)
40. L. Ji, J. Wang, X. Teng et al., N, P-Doped Molybdenum carbide nanofibers for efficient hydrogen production. *ACS Appl. Mater. Inter.* **10**, 14632 (2018)
41. X.F. Lu, L. Yu, J. Zhang et al., Ultrafine dual-phased carbide nanocrystals confined in porous nitrogen-doped carbon dodecahedrons for efficient hydrogen evolution reaction. *Adv. Mater.* **31**, 1900699 (2019)
42. J. Xie, S. Li, X. Zhang et al., Atomically-thin molybdenum nitride nanosheets with exposed active surface sites for efficient hydrogen evolution. *Chem. Sci.* **5**, 4615 (2014)
43. B. Cao, G.M. Veith, J.C. Neuefeind et al., ChemInform abstract: mixed close-packed cobalt molybdenum nitrides as non-noble metal electrocatalysts for the hydrogen evolution reaction. *ChemInform* **45**, 19186 (2014)
44. H. Fan, H. Yu, Y. Zhang et al., Fe-Doped Ni<sub>3</sub>C Nanodots in N-doped carbon nanosheets for efficient hydrogen-evolution and oxygen-evolution electrocatalysis. *Angew. Chem. Int. Ed.* **56**, 12566 (2017)
45. J. Guan, C. Li, J. Zhao et al., FeOOH-enhanced bifunctionality in Ni<sub>3</sub>N nanotube arrays for water splitting. *Appl. Catal. B.* **269**, 118600 (2020)
46. X. Shu, S. Chen, S. Chen et al., Cobalt nitride embedded holey N-doped graphene as advanced bifunctional electrocatalysts for

- Zn-Air batteries and overall water splitting. *Carbon* **157**, 234 (2019)
47. L. Jiang, J. Duan, J. Zhu et al., Iron-cluster-directed synthesis of 2D/2D Fe-N-C/MXene Superlattice-like heterostructure with enhanced oxygen reduction electrocatalysis. *ACS Nano* **14**, 2436 (2020)
  48. P. Zhang, S. Xie, P. Deng et al., Oxygen-Deficient NiCo<sub>2</sub>O<sub>4</sub> nanowires as the robust cathode for high-performance nickel-zinc batteries. *J. Mater. Res.* (2022). <https://doi.org/10.1557/s43578-022-00512-6>
  49. G.L. Li, S. Cao, Z.F. Lu et al., FePc nanoclusters modified NiCo layered double hydroxides in parallel with Ti<sub>3</sub>C<sub>2</sub> MXene as a highly efficient and durable bifunctional oxygen electrocatalyst for zinc-air batteries. *Appl. Surf. Sci.* **519**, 153142 (2022)
  50. Q. Wang, L. Shang, R. Shi et al., NiFe layered double hydroxide nanoparticles on Co, N-Codoped carbon Nanoframes as efficient bifunctional catalysts for rechargeable zinc-air batteries. *Adv. Energy Mater.* **7**, 2 (2017)
  51. X. Zhang, Y. Zhang, H. Huang et al., Electrochemical fabrication of shape-controlled Cu<sub>2</sub>O with spheres, octahedrons and truncated octahedrons and their electrocatalysis for ORR. *New J. Chem.* **42**, 458 (2018)
  52. Y. He, X.P. Han, D.W. Rao et al., Charge redistribution of Co on cobalt (II) oxide surface for enhanced oxygen evolution electrocatalysis. *Nano Energy* **61**, 267 (2019)
  53. S. Li, Z. Li, R. Ma et al., A glass-ceramic with accelerated surface reconstruction toward the efficient oxygen evolution reaction. *Angew. Chem. Int. Ed. Engl.* **60**, 3773 (2021)
  54. Y. Kang, S. Wang, S. Zhu et al., Iron-modulated nickel cobalt phosphide embedded in carbon to boost power density of hybrid sodium-air battery. *Appl. Catal. B-Environ.* **285**, 15 (2021)
  55. P.S. Arunkumar, P. Siva, R. Naveenkumar et al., Enhanced discharge capacity of Mg-air battery with addition of water dispersible nano MoS<sub>2</sub> sheet in MgCl<sub>2</sub> electrolyte. *Ionics (Kiel)*. **25**, 583 (2018)
  56. M.K. Puglia, M. Malhotra, A. Chivukula et al., "Simple-Stir" Heterolayered MoS<sub>2</sub>/Graphene Nanosheets for Zn-Air Batteries. *ACS Appl. Nano Mater.* **4**, 10389 (2021)
  57. Q. Hong, H. Lu, Y. Cao, Improved oxygen reduction activity and stability on N, S-enriched hierarchical carbon architectures with decorating core-shell iron group metal sulphides nanoparticles for Al-air batteries. *Carbon* **145**, 53 (2019)
  58. J.Y. Zhao, R. Wang, S. Wang et al., Metal-organic framework-derived Co<sub>9</sub>S<sub>8</sub> embedded in N, O and S-tridoped carbon nanomaterials as an efficient oxygen bifunctional electrocatalyst. *J. Mater. Chem. A*. **7**, 7389 (2019)
  59. R. Singhal, M. Chaudhary, S. Tyagi et al., Recent developments in transition metal-based nanomaterials for supercapacitor applications. *J. Mater. Res.* (2022). <https://doi.org/10.1557/s43578-022-00598-y>
  60. N. Feng, R. Meng, L. Zu et al., A polymer-direct-intercalation strategy for MoS<sub>2</sub>/carbon-derived heteroaggregates with ultrahigh pseudocapacitance. *Nat Commun.* **10**, 1372 (2019)
  61. D.J. McPherson, A. Dowd, M.D. Arnold et al., Electrochemical energy storage on nanoporous copper sponge. *J. Mater. Res.* (2022). <https://doi.org/10.1557/s43578-022-00535-z>
  62. Y. Zhou, K. Maleski, B. Anasori et al., Ti<sub>3</sub>C<sub>2</sub>T<sub>x</sub> MXene-reduced graphene oxide composite electrodes for stretchable supercapacitors. *ACS Nano* **14**, 3576 (2020)
  63. I. Hussain, C. Lamiel, S.G. Mohamed et al., Controlled synthesis and growth mechanism of zinc cobalt sulfide rods on Ni-foam for high-performance supercapacitors. *J. Ind. Eng. Chem.* **71**, 250 (2019)
  64. S. Rao, I. Kanaka Durga, B. Naresh et al., One-pot hydrothermal synthesis of novel Cu-MnS with PVP cabbage-like nanostructures for high-performance supercapacitors. *Energies* **11**, 1590 (2018)
  65. S.K. Balasingam, A. Thirumurugan, J.S. Lee et al., Amorphous MoS<sub>x</sub> thin-film-coated carbon fiber paper as a 3D electrode for long cycle life symmetric supercapacitors. *Nanoscale* **8**, 11787 (2016)
  66. J. Li, R. Wu, X. Yang, MoS<sub>2</sub> modified TiN nanotube arrays for advanced supercapacitors electrode. *Physica E*. **118**, 113951 (2020)
  67. Y. Zhuo, E. Prestat, I.A. Kinloch et al., Self-assembled 1T-MoS<sub>2</sub>/functionalized graphene composite electrodes for supercapacitor devices. *ACS Appl. Energ. Mater.* **5**, 61 (2022)
  68. R.B. Rakhi, B. Ahmed, D. Anjum et al., Direct chemical synthesis of MnO<sub>2</sub> nanowhiskers on transition-metal carbide surfaces for supercapacitor applications. *ACS Appl. Mater. Inter.* **8**, 18806 (2016)
  69. C. Chen, Y. Kang, Z. Huo et al., Highly crystalline multimetallic nanoframes with three-dimensional electrocatalytic. *Sci.* **343**, 1339 (2014)
  70. D. Wang, H.L. Xin, R. Hovden et al., Structurally ordered intermetallic platinum-cobalt core-shell nanoparticles with enhanced activity and stability as oxygen reduction electrocatalysts. *Nat. Mater.* **12**, 81 (2013)
  71. K.P. Singh, E.J. Bae, J.S. Yu, Fe-P a new class of electroactive catalyst for oxygen reduction reaction. *J. Am. Chem. Soc.* **137**, 3165 (2015)
  72. S. Dou, L. Tao, J. Huo et al., Etched and doped Co<sub>9</sub>S<sub>8</sub>/graphene hybrid for oxygen electrocatalysis. *Energy Environ. Sci.* **9**, 1320 (2016)
  73. H.F. Wang, C. Tang, B. Wang et al., Bifunctional transition metal hydroxysulfides: room-temperature sulfurization and their applications in Zn-Air batteries. *Adv. Mater.* **29**, 3254 (2017)
  74. T. Varga, G. Ballai, L. Vászárhelyi et al., Co<sub>4</sub>N/nitrogen-doped graphene: A non-noble metal oxygen reduction electrocatalyst for alkaline fuel cells. *Appl. Catal. B-Environ.* **237**, 826 (2018)

75. Z. Rui, Y. Yao, F. Xinran et al., Nonprecious transition metal nitrides as efficient oxygen reduction electrocatalysts for alkaline fuel cells. *Sci. Adv.* **8**, 1584 (2022)
76. K.A. Stoerzinger, M. Risch, B. Han et al., Recent insights into manganese oxides in catalyzing oxygen reduction kinetics. *ACS Catal.* **5**, 6021 (2015)
77. Y.C. Zhang, S. Ullah, R. Zhang et al., Manipulating electronic delocalization of  $Mn_3O_4$  by manganese defects for oxygen reduction reaction. *Appl. Catal. B-Environ.* **277**, 119247 (2020)
78. L. Ma, S. Chen, Z. Pei et al., Flexible Waterproof Rechargeable Hybrid Zinc Batteries Initiated by Multifunctional Oxygen Vacancies-Rich Cobalt Oxide. *ACS Nano* **12**, 8597 (2018)
79. M. Xiao, J. Zhu, L. Feng et al., Meso/macroporous nitrogen-doped carbon architectures with iron carbide encapsulated in graphitic layers as an efficient and robust catalyst for the oxygen reduction reaction in both acidic and alkaline solutions. *Adv. Mater.* **27**, 2521 (2015)
80. E.C. Weigert, M.B. Zellner, A.L. Stottlemeyer et al., A combined surface science and electrochemical study of tungsten carbides as anode electrocatalysts. *Top. Catal.* **46**, 349 (2007)
81. T. Sheng, X. Lin, Z.Y. Chen et al., Methanol electro-oxidation on platinum modified tungsten carbides in direct methanol fuel cells: a DFT study. *Phys. Chem. Chem. Phys.* **17**, 25235 (2015)
82. K.T. Lee, Y.S. Jung, S.M. Oh, Synthesis of tin-encapsulated spherical hollow carbon for anode material in lithium secondary batteries. *J. Am. Chem. Soc.* **7**, 151 (2003)
83. Y.P. Wu, E. Rahm, R. Holze, Carbon anode materials for lithium ion batteries. *J. Power. Sources.* **114**, 228 (2003)
84. L. Ji, Z. Lin, M. Alcoutlabi et al., Recent developments in nanostructured anode materials for rechargeable lithium-ion batteries. *Energy Environ. Sci.* **4**, 2682 (2011)
85. S. Fang, D. Bresser, S. Passerini, Transition metal oxide anodes for electrochemical energy storage in lithium- and sodium-ion batteries. *Adv Energy Mater.* **10**, 1 (2019)
86. J. Luo, J. Liu, Z. Zeng et al., Three-dimensional graphene foam supported  $Fe_3O_4$  lithium battery anodes with long cycle life and high rate capability. *Nano Lett.* **13**, 6136 (2013)
87. E. Larson, L. Williams, C. Jin et al., Molybdenum oxide nanoporous asymmetric membranes for high capacity lithium ion battery anode. *J. Mater. Res.* (2021). <https://doi.org/10.1557/s43578-021-00347-7>
88. B. Liu, J. Zhang, X. Wang et al., Hierarchical three-dimensional  $ZnCo_2O_4$  nanowire arrays/carbon cloth anodes for a novel class of high-performance flexible lithium-ion batteries. *Nano Lett.* **12**, 3005 (2012)
89. Z. Yu, X. Qu, A. Dou et al., Carbon-coated cation-disordered rocksalt-type transition metal oxide composites for high energy Li-ion batteries. *Ceram. Int.* **47**, 1758 (2021)
90. X. Gao, L. Xiong, J. Wu et al., Scalable and controllable synthesis of 2D high-proportion 1T-phase  $MoS_2$ . *Nano Res.* **13**, 2933 (2020)
91. L. Huang, Z. Hu, H. Jin et al., Salt-assisted synthesis of 2D materials. *Adv. Funct. Mater.* **30**, 1908486 (2020)
92. G. Kalimuldina, I. Taniguchi, High performance stoichiometric  $Cu_2S$  cathode on carbon fiber current collector for lithium batteries *Electrochim. Acta.* **224**, 329 (2017)
93. Y. Xiao, J.Y. Hwang, I. Belharouak et al., Superior Li/Na-storage capability of a carbon-free hierarchical  $CoS_x$  hollow nanostructure. *Nano Energy* **32**, 320 (2017)
94. M.G. Fayed, S.Y. Attia, Y.F. Barakat et al., Carbon and nitrogen co-doped  $MoS_2$  nanoflakes as an electrode material for lithium-ion batteries and supercapacitors. *Sustain. Mater. Technol.* **29**, e00306 (2021)
95. L. Lai, J. Zhu, B. Li et al., One novel and universal method to prepare transition metal nitrides doped graphene anodes for Li-ion battery. *Electrochim. Acta.* **134**, 28 (2014)
96. C.H. Wang, N. Kurra, M. Alhabet et al., Titanium carbide (MXene) as a current collector for lithium-ion batteries. *ACS Omega* **3**, 12489 (2018)